Calorimetric and Dynamic Light-Scattering Investigation of Cationic Surfactant−DNA Complexes

S. Marchetti

Dipartimento di Fisica, Universita' di Firenze, Via G. Sansone, I-50019 Sesto Fiorentino, Firenze, Italy

G. Onori

Dipartimento di Fisica, Universita' di Perugia, Via A. Pascoli, I-06100 Perugia, Italy, CEMIN (Centro di Eccellenza Materiali Innovativi Nanostrutturati per le Applicazioni Chimiche, Fisiche e Biomediche) and INFM CRS-SOFT

C. Cametti*

Dipartimento di Fisica, Universita' di Roma "La Sapienza" Piazzale A. Moro 5, I-00185 - Rome, Italy, and INFM CRS-SOFT, Unita' di Roma 1

Received: June 9, 2006; In Final Form: September 7, 2006

By means of combined calorimetric and dynamic light-scattering measurements, we have investigated the conformational behavior of DNA chains after thermal melting in the presence of a cationic surfactant at different concentrations, up to a surfactant-to-phosphate group molar ratio close to unity. Both the specific heat capacity, C_P^{ex}, and the hydrodynamic radius R of the DNA chains provide support for the existence of two structural arrangements with different thermal stabilities, coexisting in the bulk solution. Although a component remains an elongated unfolded DNA chain originated in the thermal denaturation, the second component, consisting of DNA−surfactant complexes, assumes a compact structure with an average size of about 80 nm, whose thermal denaturation occurs at temperatures higher than 100 °C.

1. Introduction

The conformational behavior of DNA molecules in the presence of certain ionic or zwitterionic solutes or in mixed organic−aqueous solvents has been studied extensively in recent years,[1,2] for both its technological and biomedical importance. In fact, since the development of methods for DNA extraction and purification and, lately, for the potential use of these systems as vehicles for gene delivery and gene transfection, a number of studies on the compaction of DNA by cationic species in bulk solution have been appeared. In particular, the interactions between DNA and cationic surfactants have received particular attention because of their significance in biomedical applications, as well as for a better understanding of DNA behavior in living cells.[3−5]

Interactions of a single chain surfactant such as cetyltrimethylammonium bromide (CTAB) with calf thymus DNA (ctDNA) have been investigated by various physical methods[7−10] and, recently, these interactions have been also studied at the single-molecule level, with the use of a fluorescence microscopy technique.[11,12] CTAB is an effective compacting agent for DNA.[13] It has been found that isolated DNA chains undergo a discrete coil−globule transition upon the increase of the concentration of the surfactant in the solution. This process starts at very low concentrations of the cationic surfactant, well below its critical micelle concentration (cmc).

Cationic surfactants interact with DNA by a combination of initial electrostatic interactions followed by a cooperative binding of surfactant ligands to the same DNA molecule, driven by hydrophobic forces.[11,14] This means that, at submicellar concentrations of surfactant, free/unbound DNA chains coexist with surfactant-saturated DNA chains. The existence of a bimodal size distribution between an elongated coil and a compact globule state has been also confirmed in our recent work,[15] where the compaction of ctDNA by CTAB has been investigated by means of combined viscosity and dynamic light-scattering (DLS) measurements. Similar investigations were carried out by Cardenas et al.,[6] who used DLS to study surfactant-induced compaction of high-molecular-weight DNA that undergoes a transition evidenced by the decrease of the hydrodynamic radius from about 100 nm to about 50 nm, in the presence of CTAB surfactant.

DLS measurements provide a direct observation of the surfactant-induced conformational changes of a single DNA molecule because this technique probes changes in the translational diffusion coefficient from the elongated coil state to the compact globule state, induced by the addition of the surfactant. The use of the DLS technique allowed us to observe the coil−globule coexistence in bulk, in a direct way, supporting evidence that the transition between the two states, elongated coil and compact globule, is a cooperative process, when it is observed in the macroscopic ensemble of DNA chains, but it is not continuous and occurs in discrete steps for each DNA molecule.

Although there is plenty of literature about compaction of DNA with cationic surfactants,[7−10] less attention has been paid to the DNA structural transition with temperature, in the presence of amphiphiles. The coexistence of the coil and globular forms of DNA in a certain surfactant concentration

* Corresponding author. E-mail: cesare.cametti@roma1.infn.it.

10.1021/jp063598r CCC: $33.50
Published on Web 11/14/2006

interval could be more directly revealed by calorimetric methods, if the two forms have a different thermal stability. Actually, UV melting experiments have clearly shown the stabilization of the DNA duplex by cationic surfactants.[9,16]

However, a number of problems about the thermodynamics of binding of simple cationic amphiphiles to DNA have not been addressed so far and, for a better understanding of the characteristic of the CTAB−DNA interactions, it is necessary to investigate whether or not conformational changes occur in the double helix of DNA upon binding cationic surfactant. No report is, until now, available, to our knowledge, using differential scanning microcalorimetry (DSC) as an experimental technique to study the effect of cationic surfactants on the thermal stability of high-molecular-weight DNA.

In the present work, the thermal melting of ctDNA was investigated in the presence of varying concentrations of CTAB by means of DSC. The behavior of the hydrodynamic radius and the size distribution of the ctDNA/CTAB complexes before and after the melting of DNA has been studied by means of DLS measurements. Circular dichroism (CD) measurements were also made on the solution of ctDNA in the presence of CTAB in order to examine the possibility that conformational changes occur upon binding of CTAB to the DNA.

The aim of this study, based on the combined use of differential scanning microcalorimetry (DSC), dynamic light scattering (DLS), and circular dichroism measurements (CD), was to obtain information on the stability of DNA in the ctDNA/CTAB complexes and to support further evidence for the coexistence of two different forms of DNA in dilute aqueous solutions, at submicellar surfactant concentrations.

2. Experimental Section

2.1. Materials. Calf thymus DNA (sodium salt, ctDNA) was purchased from Sigma Chem. Co. Stock solution of DNA was prepared by dissolving commercial nucleic acid in 10 mM NaCl aqueous solution and fragmented by sonic vibration with a Vibra Cell sonifier by Sonic and Materials Inc. (5 mg/mL concentration, 1 min sonication time), in order to obtain DNA fragments shorter and with a narrower size distribution than those of the original commercial sample. The molecular weight distribution of DNA fragments was determined by means of agarose gel electrophoresis, yielding values between 0.5 and 1 kbp. The molecular weight of the samples investigated was in the range from 3.3 to 6.6×10^{-5} g/mol with a fragment length distribution between 0.2 and 0.4×10^{-6} m. The stock solution was diluted with 10 mM NaCl aqueous solution. The final concentration of nucleic acid was 0.1 mM in terms of phosphate groups and this value was maintained constant in CD, DLS, or DSC measurements. The DNA concentration was calculated according to the absorbance at 260 nm by using $\epsilon_{DNA} = 6600\ M^{-1}\ cm^{-1}$. The CTAB surfactant was from Fluka and was used without further purification. The solutions were prepared by weighing. In all of the experiments, the DNA concentration was maintained constant while the concentration of CTAB was varied from 0 to 0.15 mM, changing the surfactant-to-DNA molar ratio, $X = [CTAB]/[PO_4^-]$ from 0 to about 1.5.

The CTAB concentrations employed are much below the critical micelle concentration (about 0.92 mM, as inferred by surface tension measurements) and, hence, the binding of CTAB to ctDNA occurs, under these conditions, predominantly in the monomeric form and not in the micellar form. The pH of the DNA and CTAB solutions, measured by means of a Crison micropH model 2000 before and after the mixing, was about 7 and no appreciable changes were observed in time, after the mixing.

2.2. CD Measurements. Circular dichroism (CD) spectra were collected with 1-cm-path-length rectangular quartz cell at 25 °C using a Jasco J-810 spectropolarimeter equipped with a Peltier temperature control device. CD spectra were expressed as molar ellipticity, $[\theta]$ (mdeg cm^2 $dmol^{-1}$). Spectra were typically recorded in the range of 200−320 nm with 0.1 nm resolution and were signal-averaged by adding at least three different scans. The baseline was corrected by subtraction of the appropriate 10 mM NaCl aqueous solution spectrum.

2.3. DSC Measurements. Differential scanning calorimetry (DSC) measurements were carried out using a micro-DSC II Setaram (Lyon, France) with 1.0 mL calorimetric cell volume. The heating scan rate was 0.50 °C/min, starting from 25 °C up to 100 °C. The total mass of the measured sample was 0.85 g. The weights of the reference and sample cell were always matched. The raw data were converted to an apparent molar heat capacity by correcting for the instrumental calibration curve and by dividing each data point by the scan rate and the number of moles of base pairs in the sample cell.

In order to minimize systematic differences between the measuring and reference cell, after the subtraction of the scan of the solvent versus solvent from the power input scan of the DNA solution versus solvent, we obtained the value of the excess heat capacity function, C_P^{ex}, per mole of base pairs, according to the Freire and Biltonen procedure.[18,19]

The total calorimetric enthalpy of denaturation, ΔH, was obtained by integration of the area enclosed by the transition curve and the pre- and post-transition baseline. The melting temperature, T_m, was determined as midpoint of the melting transition.

2.4. DLS Measurements. The size and size distribution of DNA and DNA−CTAB complexes have been characterized by means of the dynamic light-scattering technique,[20] by measuring, at the wavelength 632.8 nm and at a scattering angle of 90°, the normalized time autocorrelation function of the intensity of the scattered light $g^{(2)}(q, \tau)$ that can be expressed through the normalized electric field correlation function, $g^{(1)}(q, \tau)$, according to $g^{(2)}(q, \tau) = A[1 + \beta|g^{(1)}(q,\tau)|^2]$. For a dilute suspension of polydisperse particles, the correlation function $g^{(1)}(q, \tau)$ deviates from a single-exponential decay and can be written as the Laplace transform of a continuous distribution $G(\Gamma)$

$$g^{(1)}(\tau) = \int_0^\infty G(\Gamma) \exp(-\Gamma\tau)\, d\Gamma \qquad (1)$$

The analysis of the decay time distribution has been carried out by the inverse Laplace transformation by means of a fit routine CONTIN,[21] which employs the constrained regularization method.

3. Results and Discussion

3.1. CD Measurements. CD experiments were performed on solution of ctDNA in the presence of varying amounts of CTAB in order to determine if secondary structural changes occur upon binding of CTAB to DNA. The CD spectrum in the UV range is a technique very sensitive to the conformational change of the helix, providing information on the possible different binding reactions occurring in the system.[22] The UV circular dichroic spectrum of ctDNA exhibits a positive band at 275 nm, due to the base stacking, and a negative band at 245 nm, due to the helicity of B-DNA and a crossover around 258 nm, corresponding to the wavelength maximum for normal absorption, as shown in Figure 1.

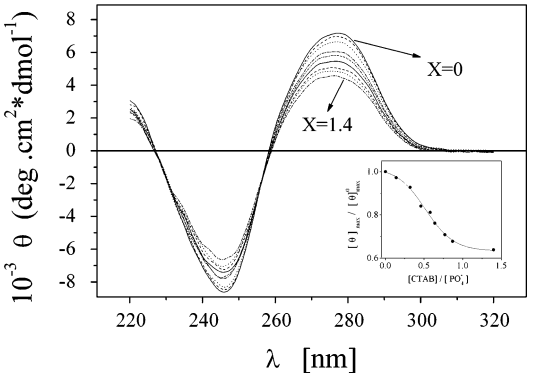

Figure 1. CD spectra of ctDNA at various molar ratios, *X*, in 10 mM NaCl aqueous solutions (pH = 7.0). In the inset, the intensity of the positive band at 275 nm as a function of *X* normalized to $X = 0$ is shown.

Upon the incremental addition of CTAB to DNA at pH 7, a slight decrease in the intensity of both the 275 nm positive band and the 245 nm negative band are observed. However, the overall contour of the spectrum is maintained and there is no major change in conformation of the DNA structure as CTAB binds to the duplex.

In general, changes in the intensity of the CD peak at 275 nm have been associated with alteration of hydration of the helix in the vicinity of phosphate or the ribose ring, as the ionic concentrations are changed.[23,24] Probably, exchanging a cationic lipid, such as CTAB, with a sodium ion in the counterion cloud around DNA would lead to a change in hydration near the phosphate groups of the DNA helix, particularly because the alkyl chain of the surfactant is quite hydrophobic.[22,25,26]

In the inset of Figure 1, the intensity of the positive band at 275 nm as a function of the surfactant-to-phosphate group molar ratio $X = [CTAB]/[PO_4^-]$, normalized to the intensity at $X = 0$, is reported. As can be seen, this quantity decreases rather steeply as *X* increases, reaching a saturation value at approximately $X = 1$. This result indicates the crucial role played by electrostatic interactions in the complex formation between the positively charged trimethylammonium group of CTAB and the backbone phosphate group of DNA, being in good agreement with previously reported data. For example, Mel'nikov et al.[11] studied the binding of CTAB to DNA by a potentiometric titration method and it was possible, from these data, to obtain the binding isotherm. These results indicate a cooperative binding process, the binding isotherm showing the typical sigmoidal shape, and these authors found that the slope of the isotherm decreases toward zero, at the ratio $X = [CTAB]/[PO_4^-]$ close 0.8.

3.2. DSC Measurements. In order to study the effect of CTAB surfactant on the stability of DNA on the DNA/CTAB complex, the thermal melting of ctDNA was investigated by DSC measurements, in the presence of varying concentrations of CTAB. DNA melting is the endothermic process of separating the two strands wound in a double helix into two single strands. Basically, this phenomenon is similar to the much more studied protein unfolding. In both cases, the macromolecule cooperatively loses its secondary structure and exposes a large fraction of its internal surface to the aqueous solution.

Figure 2 shows specific heat capacity, at constant pressure, C_p^{ex}, as a function of temperature, in some selected different environments. Panel A shows C_p^{ex} for 10 mM NaCl aqueous solution of ctDNA at pH = 7.0. Panels B−D show C_p^{ex} for ctDNA in the presence of CTAB at three selected values of *X*. The overwhelming predominance of the next nearest-neighbor

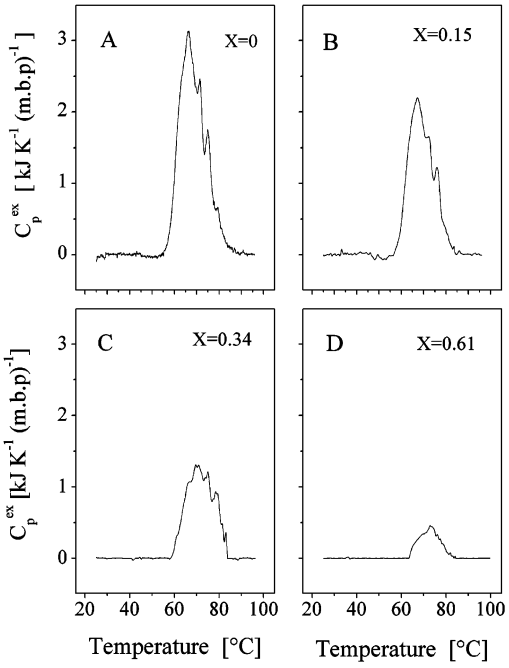

Figure 2. Melting profile of ctDNA in 10 mM NaCl aqueous solution at pH = 7.0 in the absence (panel A) and in the presence of CTAB at three selected values of *X* (panels B−D). The specific heat capacity, at constant pressure, C_P^{ex} is expressed for unit of mole base pairs (mbp).

interaction along each particular sequence makes unique the heat capacity as a function of temperature, for each DNA sequence.

The dependence of a melting curve of DNA upon its content is well-known. The main effect of DNA composition on the double-helix stability is due to the large enthalpy difference (∼1000 cal/mol) between GC and AT base pairs, coming from the extra hydrogen bond in the former. As a consequence, GC-rich DNA melts at a higher temperature than AT-rich DNA.

The thermal profile of ctDNA (Figure 2A) exhibits an asymmetrical melting band with, at least, four sub-transitions, starting from the top of the principal maximum and descending on the high-temperature slope of the basic denaturation curve.[31,32] As established, the individual peak that occurred at different temperatures is due to the difference in the base composition and covers different areas because of the relative frequency of the particular repetitive sequences in terms of different GC content (42% for our calf thymus DNA).[33]

After the scanning, the samples were cooled down and re-scanned by means of DSC measurements. Because no peak appeared in the second run and the corresponding thermal profile is completely flat, we can conclude that the denaturation process is almost completely irreversible.

Figure 2, panels B−D, shows how the melting curve of ctDNA changes with the increase in CTAB concentration, in the amphiphile−DNA mixture. As can be seen, a slight increase of the temperature at the midpoint of the melt, T_m, and a dramatic and progressive decrease of the calorimetric enthalpy, ΔH, that is, the area enclosed by the transition curve and the pre- and post-transition baseline, (practically zero at $X \simeq 0.8$), are observed.

However, no substantial modifications of the typical profile of ctDNA with the increase of CTAB concentration are evidenced, so the "fine structure" of the native DNA melting curve is entirely presented in DNA−amphiphile complex solutions. The trend of $\Delta H/\Delta H_0$ as a function of *X* (Figure 3) clearly demonstrates the existence of a transition that falls in

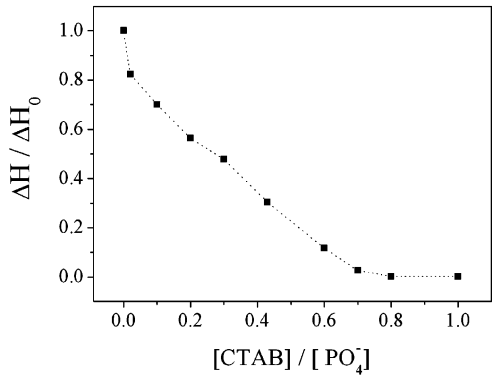

Figure 3. Dependence of the calorimetric enthalpy (ΔH) normalized to $X = 0$ as a function of the surfactant-to-phosphate group molar ratio, X.

the same range of X, as the one revealed by CD, DLS,[15] and potentiometric titration.[9]

The isothermal titration calorimetry and light-scattering measurements used by Spink at al.[9] to study the thermodynamics and the configurational aspects of the interaction confirm this trend. From our point of view, for interpreting the overall observed phenomenology, it is necessary to suggest the formation of a second species that is thermally more stable than the initially observed one, whose thermal denaturation is over 100 °C, out of the temperature range allowed by our experimental setup.

3.3. DLS Measurements. In order to verify this hypothesis, we have carried out DLS measurements on ctDNA−CTAB complexes after thermal denaturation. Each sample, at different CTAB concentrations, was first progressively heated (scan rate 10 °C/h) in a thermostatted bath in the range from 25 to 100 °C, within the accessible temperature threshold of the experimental setup. At the end of the melting process, we obtain the thermal profile shown in Figure 2. Each sample was maintained at the temperature of 100 °C for 1 h and then the sample was progressively cooled down, with the same warming scan rate, to 25 °C, the temperature at which the light-scattering measurements were performed. A possible reassociation of the single strands during the cooling process must be discarded because of the irreversibility of the DNA denaturation, as seen by DSC measurements. Consequently, if two different DNA species with two different thermal stabilities are hypothesized, DLS measurements should evidence a bimodal size distribution, with the presence of an unfolded component and a more compact component, not influenced by the thermal treatment.

The intensity-averaged size distributions of the complexes formed by DNA and CTAB as a function of surfactant-to-DNA phosphate molar ratio X are shown in Figure 4. At $X = 0$, at the end of the heating−cooling cycle, the two strands wound in the DNA double helix are separated into two complementary single strands by thermal denaturation and only a monomodal distribution in the intensity-averaged size distribution is observed, corresponding to the translational mode of the melted DNA molecules.

With the increase of the surfactant content, we observe the presence of a bimodal distribution with the appearance of a second peak related to the more compact molecules with a smaller hydrodynamic radius of about 40 nm. With the further addition of CTAB, the amplitude of this latter component increases, while the unfolded DNA chain component decreases, until it vanishes at the charge ratio X above $X = 0.8$.

These results provide evidence for the existence of two different populations of DNA molecules in the samples investigated: one component due to elongated unfolded DNA chains and a second component due to more compact globular conformation chains.

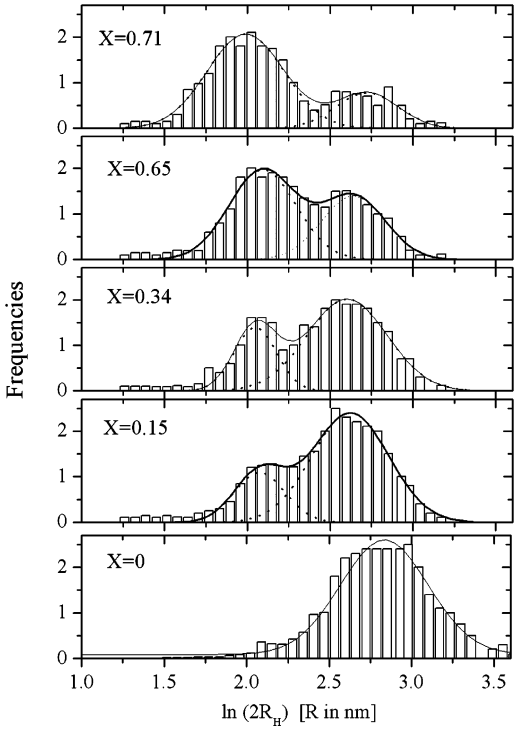

Figure 4. Size distribution of DNA−CTAB complexes as a function of the surfactant to DNA−phosphate molar charge ratio, X, at the temperature of 25 °C. Before each measurements, samples were maintained at the temperature of 100° for 1 h and then cooled down to 25 °C.

In a previous work,[15] the compaction of ctDNA induced by CTAB has been investigated by means of combined viscosity and DLS measurements, to demonstrate the formation of soluble DNA/surfactant complexes, undergoing a coil−globule transition, upon the increase of the CTAB concentration. Figure 5 shows the size distribution of the surfactant-free double-strand DNA (panel A) and of the DNA/CTAB complexes at two different charge ratios ($X = 0.55$, panel B, and $X = 1.1$, panel C). At $X = 0.55$, a bimodal distribution appears, the two populations corresponding to the free-DNA and the DNA−CTAB complexes, being characterized by different average hydrodynamic parameters. In the intermediate concentration ranges, extended DNA molecules coexist with more compacted ones. As X is further increased, above the nominal electroneutralization condition $X = 1$, the distribution tends to be monomodal, the free DNA peak disappears, and only DNA−CTAB complexes (with a more compact globular shape of about 84 nm in diameter) are present. DLS measurements on ctDNA/CTAB complexes after thermal denaturation confirm this picture and support the DSC data analysis in what concerns the stability gain of surfactant−DNA complexes. In fact, the value of about 80 nm for the hydrodynamic diameter of CTAB−DNA complexes at $X \approx 0.71$ is very close to the value observed for the same system CTAB−DNA at $X \approx 1$, without the heating−cooling cycle.

This result suggests that the size of the complex does not change, that is, in the temperature range investigated, the thermal treatment does not affect the degree of chain compaction. Temperatures higher than 100 °C seem to be necessary to denature cationic surfactant−DNA complexes. Recently, Matulis et at.[34] have developed a model for DNA−surfactant interactions

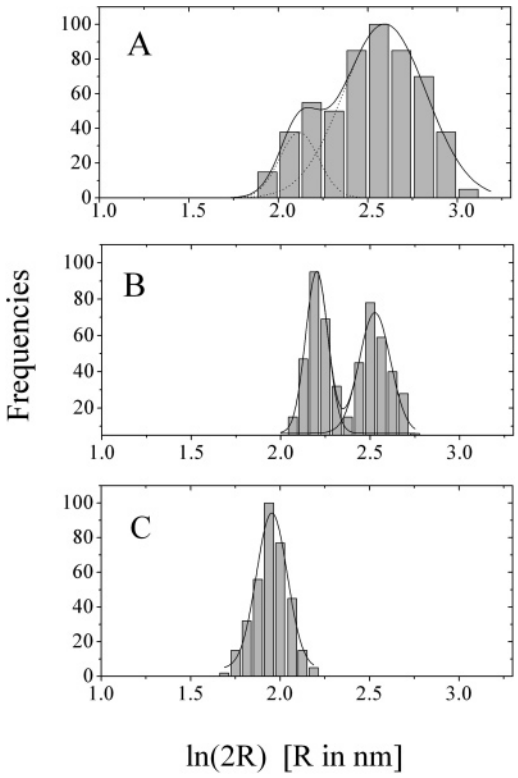

Figure 5. Size distribution of DNA−CTAB complexes (without any thermal treatment) for three different values of the surfactant to DNA−phosphate molar charge ratio, X, at a temperature of 25 °C. Panel A, $X = 0$; panel B, $X = 0.55$; panel C, $X = 1.1$.

involving the coexistence of electrostatic interactions between DNA phosphates and surfactant head groups and hydrophobic interactions between aliphatic tails. These interactions give rise to highly cooperative processes driven by a large increase in entropy and opposed by small endothermic enthalpy, at room temperature. This view is in qualitative agreement with the results presented here concerning the ability of cationic surfactants to form a thermostable DNA structure.

4. Conclusions

The surfactant-induced compaction of high-molecular-weight DNA induces a conformational change of the chain from an elongated coil state to a more compact globular state that coexists in a certain surfactant concentration range. These two components have different thermal stabilities. By means of differential scanning calorimetry and dynamic light-scattering measurements, we have investigated the thermal and hydrodynamical behavior of a cationic surfactant−DNA aqueous solution, evidencing the coexistence of two different structures. Although the surfactant-free DNA form undergoes the usual thermal stability, the surfactant-saturated DNA form assumes a rather compact globular conformation and presents a very high thermal stability, the thermal denaturation occurring at temperatures higher than 100 °C.

References and Notes

(1) Bloomfield, V. A. *Curr. Opin. Struct. Biol.* **1996**, *6*, 334−341.
(2) Lindman, B.; Thalberg, K. *Interactions of Surfactants with Polymers and Proteins*; Goddard, E. D., Ananthapadmanabhan, K. P., Eds.; CRC: Boca Raton, FL, 1993
(3) Peterson, H.; Kunath, K.; Martin, A. L; Stolnick, S.; Roberts, C. J.; Davies, M. C.; Kissel, T. *Biomacromolecules* **2002**, *3*, 926−936.
(4) Eskilsson, K.; Leal, C.; Lindman, B.; Miguel, M.; Nylander, T. *Langmuir* **2001**, *17*, 1666−1669.
(5) Chen, X.; Wang, J.; Sheu, N.; Luo, Y.; Li, L.; Liu, M.; Thomas, R. k. *Langmuir* **2002**, *18*, 6222−6228.
(6) Carednas, M.; Schillen, K.; Nylander, T.; Jansson, J.; Lindman, B. *Phys. Chem. Chem. Phys.* **2004**, *6*, 1603−1607.
(7) Wang, Z. X.; Liu, D. J.; Doug, S. J. *Biophys. Chem.* **2000**, *87*, 179−184.
(8) Cardenas, M.; Braen, A.; Nylander, T.; Lindman, B. *Langmuir* **2003**, *16*, 9577−9583.
(9) Spink, C. H.; Chaires, J. B. *J. Am. Chem. Soc.* **1997**, *119*, 10920−10928.
(10) Wagner, K.; Harries, D.; Mary, S.; Kahl, V.; Rädler, J. O.; Ben-Shaul, A. *Langmuir* **2000**, *16*, 303−312.
(11) Mel'nikov, S. M.; Sergeyev, V. G.; Yoshikawa, K. *J. Am. Chem. Soc.* **1995**, *117*, 2401−2408.
(12) Mel'nikova, Y. S.; Lindman, B. *Langmuir* **2000**, *16*, 5871−5878.
(13) Dias, R.; Mel'nikov, S.; Lindman, B.; Miguel, M. *Langmuir* **2000**, *16*, 9577−9582.
(14) Mel'nikov, S. M.; Sergeyev, V. G.; Yoshikawa, K. *J. Am. Chem. Soc.* **1995**, *117*, 9951−9956.
(15) Marchetti, S.; Onori, G.; Cametti, C. *J. Phys. Chem. B* **2005**, *109*, 3676−3680.
(16) Marky, L. A.; Patel, D.; Breslauer, K. *Biochemistry* **1981**, *20*, 1427−1431.
(17) Bonincontro, A.; Marchetti, S.; Onori, G.; Rosati, A. *Chem. Phys.* **2005**, *312*, 55−60.
(18) Freire, E.; Biltonen, R. L. *Biopolymers* **1978**, *17*, 436−79.
(19) Freire, E.; Biltonen, R. L. *Crit. Rev. Biochem.* **1978**, *5*, 85−124.
(20) Brown, W. *Dynamic Light Scattering. The Method and Some Applications*; Oxford Sci. Pub.: Oxford, 1993.
(21) Provencher, S. *Comput. Phys. Commun.* **1982**, *27*, 229−249.
(22) Carvlin, M. J.; Datta-Gupta, N.; Fiel, R. J. *Biophys. Res. Commun.* **1982**, *108*, 66−73.
(23) Hanlon, S.; Brudno, S.; Wu, T. T.; Wolf, B. *Biochemistry* **1975**, *14*, 1648−1660.
(24) Wolf, B.; Hanlon, S. *Biochemistry* **1975**, *14*, 1661−1670.
(25) Sergeyev, V. G.; Mikhailenko, S. V.; Pyshkina, O. A.; Yaminsky, I. V.; Yoshikawa, K. *J. Am. Chem. Soc.* **1999**, *121*, 1780−1785.
(26) Widom, J.; Baldwin, R. L. *J. Mol. Biol.* **1980**, *144*, 431−453.
(27) Hayakawa, K.; Santerre, J. P.; Kwak, J. C. T. *Biophys. Chem.* **1983**, *17*, 175−181.
(28) Arnott, S.; Dover, S. D.; Wonscott, A. *J. Acta Crystallogr.* **1969**, *B25*, 2192−2206.
(29) Thalberg, K.; Lindman, B.; Karlstrom, G. *J. Phys. Chem.* **1991**, *95*, 3370−3376.
(30) Thalberg, K.; Lindman, B.; Bergfalt, K. *Langmuir* **1991**, *7*, 2893−28101.
(31) Klump, H.; Volken, J.; Maeder, D.; Niemanmm, Th.; Sobolevwski, C. *Termochim. Acta* **1990**, *193*, 391−415.
(32) Mrevlishvili, G. M.; Razmadze, G.; Mdzinarashvily, T. J.; Metreveli, N. O.; Kakabodze, G. *Termochim. Acta* **1996**, *274*, 37−43.
(33) Mrevlishvili, G. M.; Kankia, B. I.; Mdzinarashvily, T. J.; Brelidze, T. I.; Khvedelidze, M. N.; Metreveli, N. O.; Razmadze, G. *Chem. Phys. Lipids* **1998**, *94*, 139−143.
(34) Matulis, D.; Rouzina, I.; Bloomfield, V. A. *J. Am. Chem. Soc.* **2002**, *124*, 7331−7342.